Model-based Scenario Optimization in Tokamaks by Integrating Free-boundary Equilibrium and Fast Transport Solvers

X. Song, Z. Wang, B. Leard, T. Rafiq, E. Schuster

Lehigh University, Bethlehem, Pennsylvania, USA

Introduction

In a recent EAST experiment, an advanced scenario called "super" improved mode (I-mode) was found to achieve a 1000-second improved confinement plasma [1]. This "super" I-mode is characterized dominantly by L-mode properties but with high confinement ($H_{98} = 1.2$), e.g., no density pedestal but with a strong electron internal transport barrier (e-ITB) associated with weak shear at the core in an unfavorable plasma configuration, providing a promising candidate operational mode for future long pulse fusion power plants. In this work, by coupling free-boundary equilibrium (FBE) and transport solvers in COTSIM [2] a model-based optimization scheme is proposed to determine the actuator trajectories needed to achieve advanced scenarios such as the "super" I-mode.

Coupling Scheme and Method

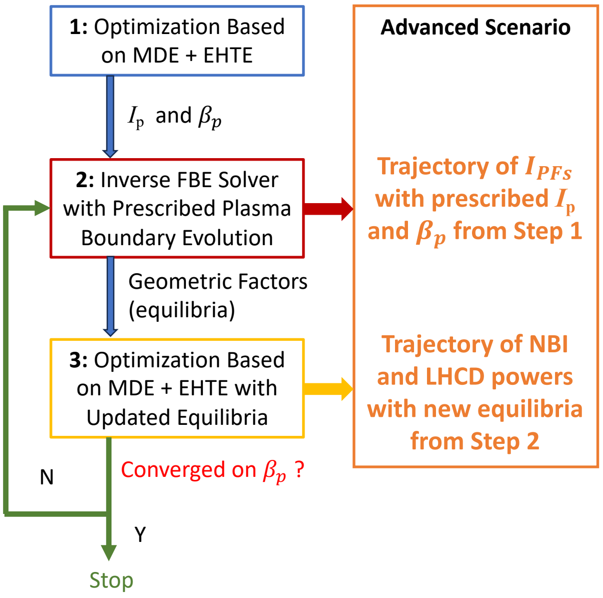

Figure 1: *COTSIM-based optimization scheme by simplified equilibrium and transport coupling.*

A FBE solver [3] has been recently implemented in COTSIM by combining the finite difference method with Picard iterations and Dirichlet boundary conditions. COTSIM enables comprehensive 1D transport simulations, integrating the magnetic diffusion equation (MDE), the electron heat transport equation (EHTE), and the 2D FBE equations. This coupling is achieved by passing the plasma equilibria computed by the FBE solver to the transport solver and returning the plasma internal profiles computed by the transport solver to the FBE solver. The optimization scheme proposed in this work implements this coupling as follows: **Step 1:** Run optimization based on MDE and EHTE with a fixed equilibrium and prescribed I_p evolution in order to achieve a target evolution of β_p. The evolution of the n_e profile is governed by a 1/2 D model while the non-inductive current driven and the heat power deposited on electrons are modeled by fixed deposition profiles computed by TRANSP [4] for an EAST L-mode scenario in combination with empirical scaling laws. The

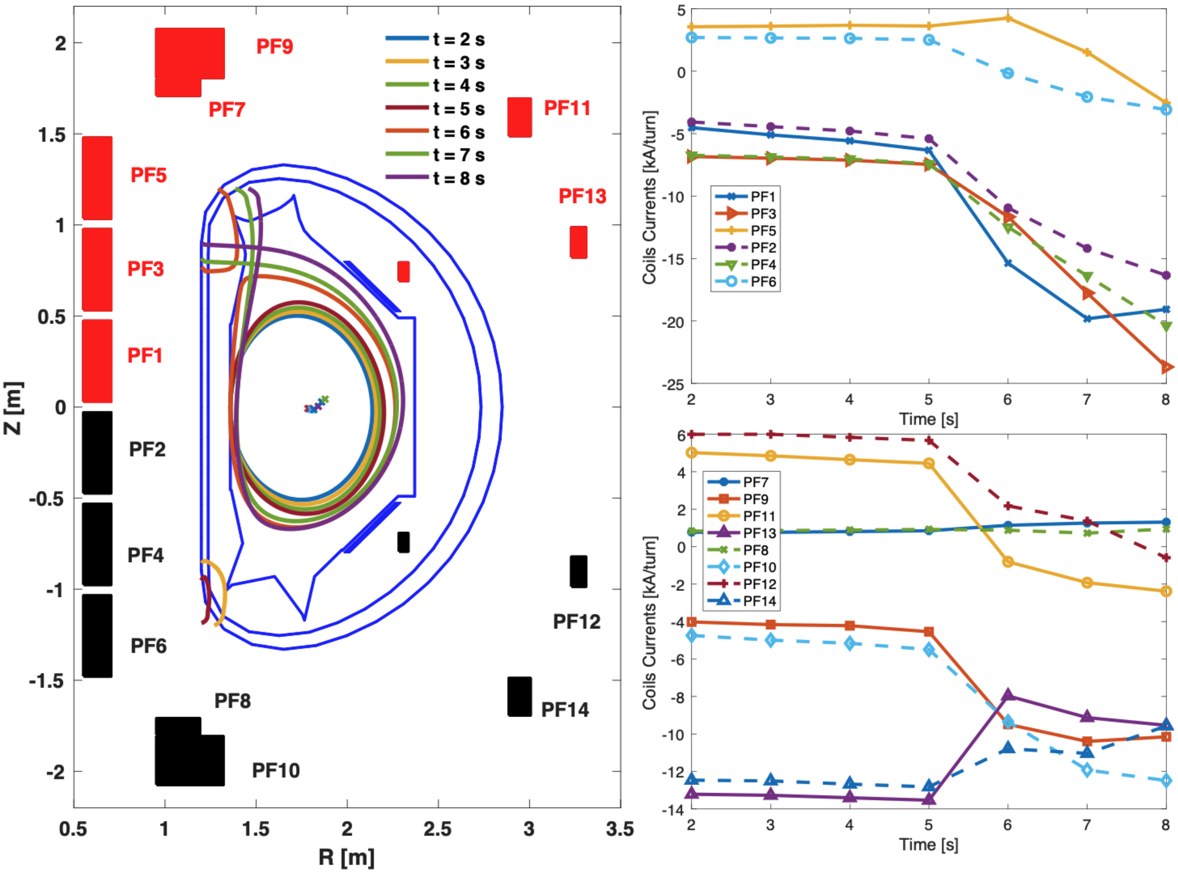

Figure 2: *Plasma boundary from limiter to divertor (USN X-point) and optimized coils currents.*

Coppi-Tang transport model [5] is adopted for the electron thermal diffusivity (χ_e) in the EHTE. **Step 2:** Run the FBE solver in inverse mode to determine the poloidal field coils currents (I_{PFs}) needed to achieve a desired evolution of the plasma boundary from limiter to divertor configuration where the final plasma shape is given by an upper single null (USN) X-point configuration, i.e., unfavorable for EAST case (fixed direction of B_0). The toroidal current density (J_ϕ) term in the right-hand-side of the Grad-Shafronov equation is parameterized by polynomial functions of the normalized poloidal flux function, ψ_N, and constrained by I_p and β_p from Step 1. The results of this step include trajectories of coils currents and plasma equilibrium parameters. **Step 3:** Run optimization with a cost function defined to achieve a weak shear at core ($\hat{\rho} = 0.1, 0.2, 0.3$) and β_p from Step 1. The MDE and EHTE are solved with the updated plasma equilibrium quantities from Step 2. The optimization ends if the difference in β_p between Steps 1 and 3 is smaller than a given tolerance. Otherwise, the optimizer returns to Step 2. The detailed work flow for the optimization is shown in Fig. 1. The final output is given by the trajectories of LHCD and NBI powers (i.e., P_{LH} and P_{NBI}) as well as of coils currents.

Optimization Results: Case Study

One objective of FBE solver running in inverse mode is to determine coil-current trajectories from ramp-up to flat-top phases in order to achieve an unfavorable magnetic configuration for a practical EAST pulse. Prescribed plasma boundaries, starting from κ=1.3 and δ=0 to κ=1.45 and δ=0.3, are provided as shown in Fig. 2 (left). The evolutions of the coils currents are also shown in Fig. 2 (right), where it is possible to note that the USN X-point is dominantly shaped by PF3, PF5, and PF9. Another objective of the FBE solver is to provide a consistent plasma-equilibrium evolution to be used in the FF optimization in Step 3 (see Fig. 1). In this way, the dynamics of the plasma equilibrium is taken into account when solving the MDE and ETHE. Consistence between I_p, β_p, and equilibrium quantities between FBE and transport (MDE and EHTE) is key in the optimization scheme. The equilibrium optmization problem (Step 2) is:

$$\min_{\Delta I_{PF,i}} \left[\sum_{j=1}^{N_{bnd}} \left\{ \sum_{i=1}^{N_{coil}} \left(G(R_j^{ref}, Z_j^{ref}; R_i, Z_i) \cdot \Delta I_{PF,i} \right) - \Delta\psi(R_j^{ref}, Z_j^{ref}) \right\}^2 + \gamma^2 \sum_{i=1}^{N_{coil}} \Delta I_{PF,i}^2 \right], \qquad (1)$$

where $\Delta\psi(R_j^{ref}, Z_j^{ref}) = \psi_{bd} - \psi(R_j^{ref}, Z_j^{ref})$, ψ_{bd} is poloidal flux function at plasma boundary, G is the Green's function with elliptic integrals, and γ is a regularization parameter. The transport optimization problem (Step 3) is stated as:

$$\min_{P_{LH}, P_{NBI}} \sum_{j=1}^{j=N_t} \left(w_t^{\rho}(t_j) \sum_{m=1}^{m=M} w_t^{\rho}(\hat{\rho}) \left(q_m(t_j) - q_m^{Tar}(t_j) \right)^2 + w_t^{\beta_p}(t_j) \left(\beta_p(t_j) - \beta_p^{Tar}(t_j) \right)^2 \right), \qquad (2)$$

where $w_t^{\rho}(t_j)$, $w_t^{\rho}(\hat{\rho})$ and $w_t^{\beta_p}(t_j)$ are weights for different time steps and $\hat{\rho}$, respectively. The pulse length for MDE and EHTE simulation starts from 1 to 9 s with an interval of 0.1 s, and the optimization occurs only at integral time steps (t = 2, 3, $\cdots$ 8 s) to save total simulation time. Numerical gradient is used to find optimized NBI and LHCD powers by the SQP method [6].

The results of the transport optimization problem are summarized in Fig. 3. Weak shear is enabled at the core by targeting a value of q = 2.1 with q_{min} larger than 1.5 to avoid localized MHD instabilities. Deviation of β_p is maintained smaller than a predefined tolerance value for the computed equilibrium evolution (Fig. 2). The optimized NBI, LHCD1 and LHCD2 powers are also shown in the figure, where power limits are strictly imposed during the optimization.

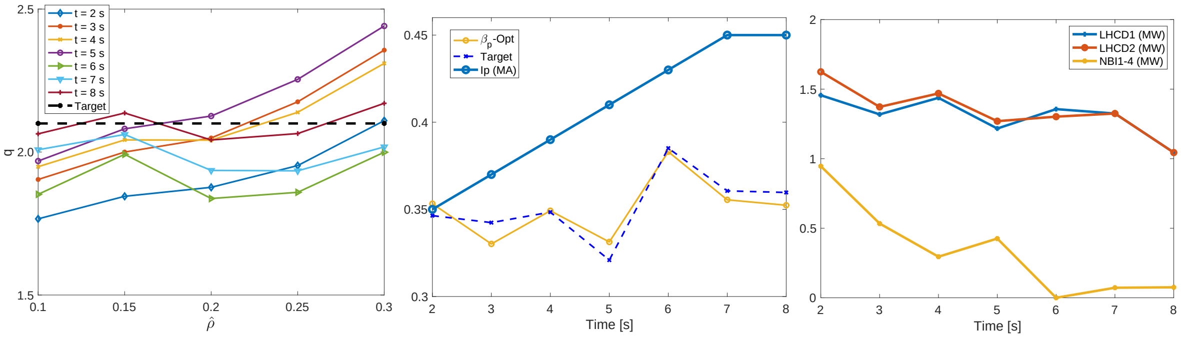

Figure 3: *Weak shear at* $\hat{\rho} = 0.1, 0.2, 0.3$ *(left),* I_p *and* β_p *(center), optimized NBI (total), LHCD1 and LHCD2 powers (right).*